

# THE VACUUM SYSTEM OF THE AUSTRALIAN SYNCHROTRON

E.Huttel, FZK, Karlsruhe, Germany

B.Barg, A.Jackson, B.Mountford, ASP, Melbourne, Australia

## Abstract

A 3 GeV Synchrotron Radiation Source is being built in Melbourne, Australia. Commissioning is foreseen in 2006. The Storage ring has a circumference of 216 m and has a 14 fold DBA structure. The vacuum chambers of the storage ring will be made from stainless steel. They consist of the e-beam chamber (width 70, height 32 mm) connected to an ante chamber, where lumped absorbers and lumped ion pumps are installed. No distributed absorbers and pumps are foreseen. The total nominal pumping speed is 31000 l/s. The vacuum chamber of each achromat will be completely assembled, baked ex situ and installed under vacuum

## BASIC DESIGN

The vacuum system of the storage ring of the Australian Synchrotron is divided into 14 arc and 14 straight section, which will house insertion devices. A top view of the vacuum chambers is given in Figure 1. An ante chamber scheme is adopted for the complete ring. The electron beam chamber has an internal width of 70 mm and a height of 32 mm. The ante chamber has the same height and a width allowing the Synchrotron Radiation propagate to lumped absorbers. Ion Pumps are installed close to these absorbers. The slot separating both

The straight chambers are formed by folding a sheet U like (including the RF shields) and the U is closed by 5 mm side sheet, too. Flanges and BPM blocks are machined from ESR 316 LN.

All longitudinal welds are e-beam welded, the transverse welds TIG are welded.

Seven BPM blocks are integrated into the vacuum chambers. The feedthroughs are welded into the block. The blocks are positioned at the entrance and the exit of the dipole, in the centre of the achromat and at the

chambers has a height of 14 mm and a width of 35 mm. Calculations for the SOLEIL vacuum chamber showed that a slot height of up to 18 mm will not contribute significantly to loss budget due to the impedance[1]. The shoulders of the slot are done for the straight chambers directly by folding the contour out of the sheets. For the dipole chamber the shoulders are made by a cooled copper bar. This will protect the chamber in the case an (helical) insertion device with horizontal field component will radiate into the vertical plane. The shield will be inserted from the entrance part and fixed with clamps to the chamber. A cross section of the vacuum chamber in the dipole and the quadrupole is given in Figure 2.

All chamber are made from 3mm stainless steel sheets (316 LN). The dipole chamber has a saw tooth structure. It is formed of an upper and lower part. The inner curved part is formed by deep drawing. The halves are directly welded together at the inner side, while the outer side is closed by a 5 mm thick side sheet. Due to its width supporting ribs are needed to keep the deflection under vacuum below 1 mm.

The upstream dipole chamber has an exit port at 0° (8 mrad from the centre of the long straight section) and a port at 7° (10°), the downstream chamber has a port at 6° (10 mrad).

beginning and the end of long straight section. The BPM blocks are used as fix points for the chambers and are mounted on same the girders as the magnets.

The four chambers constituting the arc section will have RF gate valves at both sides. This section will be completely assembled and baked ex situ and then transported under vacuum into the tunnel and mounted on the girders. The straight sections where insertions are foreseen are equipped with bellows. These sections can easily be baked in situ. The same technique was used at the SLS [2] and CLS successfully.

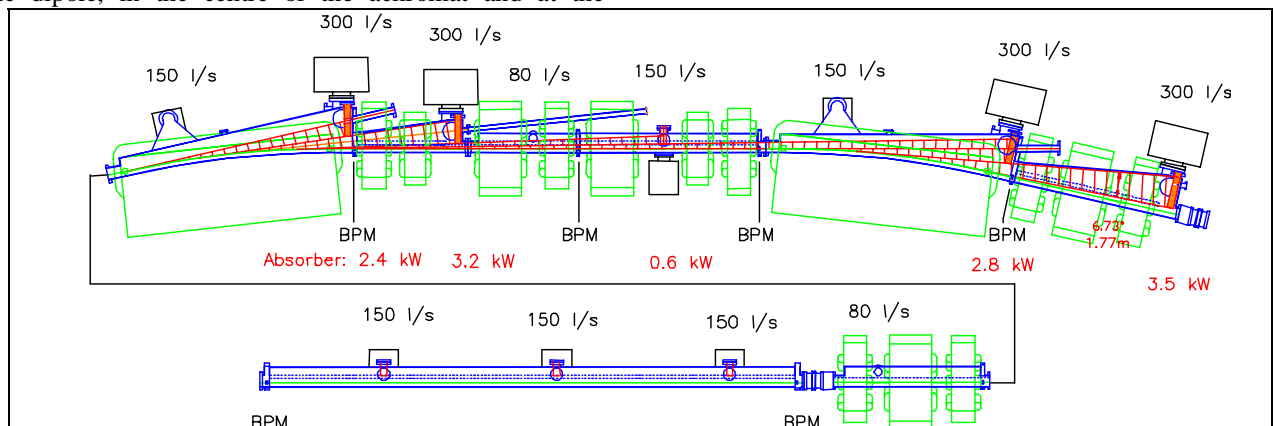


Figure 1: Top view of the vacuum system.

For the bellows the ‘double finger’ design of the PEP-II bellows is adopted, but all components made from wall of a stub, while spring fingers are providing the needed contact force [3].

The pressure will be monitored by Penning gauges (inverted Magnetron), two per arc.

### MATERIAL

Both stainless steel, copper and aluminium are used for vacuum chamber of synchrotron radiation facilities. Aluminium has an initial high desorption yield compared to copper and stainless steel but finally all materials end up with a desorption coefficient of  $10^{-6}$ .

Stainless steel is a standard material in which many manufacturers are experienced. It is more rigid compared to copper and aluminium and due to the smaller thermal expansion less sensitive to thermal distortion compared to aluminium.

Aluminium would afford stainless steel to aluminium transitions for flanges or the use of more critical aluminium flanges. Also UV tight welding is not standard.

Copper chamber have not yet been fabricated by industry. Brazing the chambers reduces the rigidity and UV tight welding can only be done by e-beam.

In order to reduce the risk and to get a more competitive offers from industry stainless steel (316 LN) was selected as material for the vacuum chamber.

### FLANGES

In order to reduce the number of bellows the four vacuum chambers within an achromat are connected without a bellow in-between. This affords a precision of the chambers and notably the flanges, which cannot be achieved easily with CF flanges. The length flange to flange are tolerated to be within  $\pm 0.2$  mm and the angle  $\pm 0.5$  mrad. Thus FlatSeal flanges are used for connecting the chambers within the arc section This allows machining of the flange faces after welding for correcting angle and length. Since this design has no gap between the flanges a low impedance is fulfilled in addition.

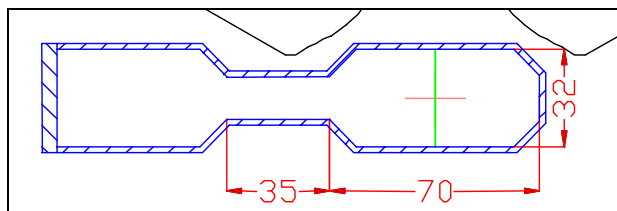


Figure 2: Cross section of the vacuum chamber within a quadrupole.

stainless steel: flexible fingers are sliding on the outside

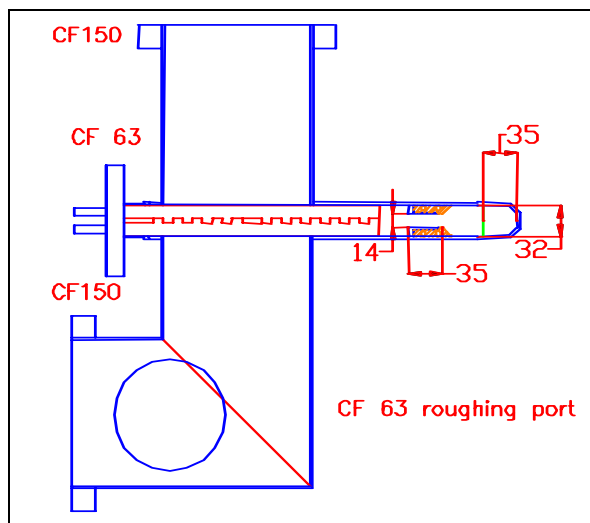


Figure 3: Cross section of the vacuum chamber in the dipole (top) and in the quadrupole.

### PUMPING

Pumping will be done by diode ion pumps. 300 l/s pumps are installed close to the main absorbers at the edge of the two saw tooth of the dipole vacuum chamber. Elsewhere 150 l/s pumps are installed in a distance of roughly 1.5 m. Standard types (Ti) will be used for the 150 l/s pumps, while (Ti-Ta) types are in discussion for the 300 l/s pumps in order to have some pumping speed for noble gases. In addition Ti sublimation pumps can be installed above of the 300 l/s pumps. These pumps will have shields to prevent Ti being sublimated into the e-beam chamber. NEG cartridges are installed at two locations, where the installation of an ion pump was not possible due to space restrictions. Overall a pumping speed of 30 000 l/s without the sublimation pumps is installed at the storage ring.

### GASLOAD AND PRESSURE DISTRIBUTION

In an electron storage ring most of the gas load is produced by SR induced desorption. The number of molecules ( $N_{mol}$ ) is proportional to the number of emitted photons.

$$N_{mol} = \eta N_{ph}$$

$$N_{ph} = 8 \cdot 10^{20} E [\text{GeV}] I [\text{A}]$$

$$Q [\text{mbar l/s}] = 4 \cdot 10^{-20} \eta N_{ph}$$

The desorption coefficient ( $\eta$ ) is dependant of the material and the accumulated photon dose. Desorption coefficient have been measured for both lumped [4] and distributed absorber [5] under lab conditions at beam lines Using these data for a more complex system of a storage ring the prediction might be less accurate. In general the desorption coefficient goes down as function of the

accumulated dose with a power of  $-0.7$  for baked system and  $-1.0$ . For the pressure calculation the following Dose dependence of the desorption coefficient was assumed for the lumped absorbers:

$$\eta = 1 \cdot 10^{-3} (10^{21} / D)^{-0.7} \quad D [\text{ph}]: \text{Photondose}$$

10 % of the photons were assumed to be equally distributed with the following dependence:

$$\eta = 1 \cdot 10^{-3} (10^{21} / d)^{-0.7} \quad d[\text{ph/m}]: \text{Photondose per meter}$$

For the calculating a MATHCAD program was written, which calculates the pressure by solving a linear equation system for a given number of pressure points : For each of these points in equilibrium the balance of the gas flow is given by:

$$P_i S_i = Q_i + \sum_j C_{ij} (P_j - P_i)$$

$$Q_i = (\sum_j C_{ij} + S_i) P_i - \sum_j C_{ij} P_j$$

Or as matrix

$$Q = M P$$

with  $M_{ij} = -C_{ij}$  for  $i \neq j$  and  $(\sum_j C_{ij} + S_i)$  for  $i = j$

which represents a linear equation system.

The pressure distributions calculated for the above assumptions and dose of 10 and 100 Ah are given in Figure 3. For an average pressure of 3 mbar (Expected for 100 Ah) the expected gas lifetime is 50h for elastic scattering, 20 h for inelastic scattering, combined 14 h.

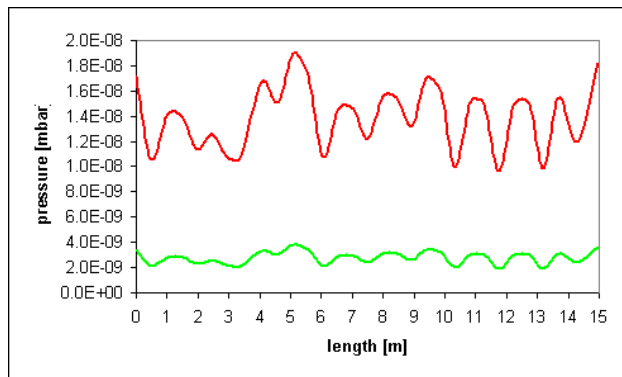


Figure 4: Expected Pressure distribution after 10 and 100 Ah.

### ABSORBER

All the Synchrotron Radiation is stopped by lumped absorbers. The total power which has to be handled by these absorbers is given by:

$$P [\text{kW}] = 88.6 E^4 [\text{GeV}] I [\text{A}] / r [\text{m}]$$

For the design values ( $E = 3 \text{ GeV}$ ,  $I = 0.2 \text{ A}$ ,  $r = 7.692 \text{ m}$ ) the total power is 187 kW.

The main absorbers are exposed up to 7 kW power with a linear power density of up to 24 W/mm. This moderate value together with its design feature allow the use of OFHC copper. ANKA-SLS design [6] is adopted. All absorbers are entered from the side wall. They consist of an upper and a lower copper block with a comb like

structure. This allows expansion when exposed to the SR and the stress is reduced compared to a solid block.. For cooling water is entering through two long cooling drills. FEM calculation in 2d have been done for a linear power density of 40 W/mm. As result a maximum temperature of  $200^\circ$  and a bulk temperature of  $90^\circ$  increase of up to  $150^\circ\text{C}$ . The load and the maximum temperature for the absorbers are given in Table 1. An increase of the stored current of up to 400 mA would be possible with the present absorber design.

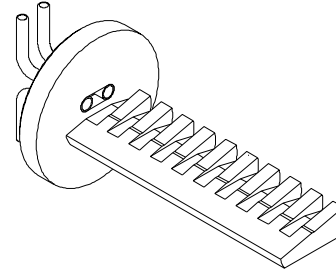


Figure 5: Lower half of the main SR absorber.

absorber	Angle [°]	Power [kW]	Linear Power [W/mm]	Max. Temp. [°C]
1	4.6	2.4	24	130
2	6.2	3.2	22	120
3	1.2	0.6	10	70
4	5.4	2.8	24	120
5	6.7	3.5	17	100
6	0.5	0.25	9	70

Table 1: Power load of the various absorbers

### REFERENCES

- [1] R.Nagaoka, 6.MAC SOLEIL, priv.com., Paris(2003)
- [2] G.Heidenreich, L.Schulz, P.Wiegand, EPAC98, Stockholm (1998) 2196
- [3] M.E.Nordby, N.Kurita, C.K.Ng, PAC95(1995)2048
- [4] V.V.Anashin, A.Bulygin, O.Malyshv, L.Mironenko, E.Pyata, V.Volkov, D.Kraemer, EPAC98, Stockholm(1998) 2163
- [5] C.Herbeaux, P.Marin, P.Rommelue, V.Baglin, O.Gröbner Vacuum 60(2001)113
- [6] S.Hermle, D.Einfeld, E.Huttel, G.Heidenreich, PAC99, New York (1999)1360